Precision Agriculture
https://doi.org/10.1007/s11119-021-09815-w

Unmanned aerial vehicle to evaluate frost damage in coffee plants

Diego Bedin Marin[1] · Gabriel Araújo e Silva Ferraz[1] · Felipe Schwerz[1] · Rafael Alexandre Pena Barata[1] · Rafael de Oliveira Faria[1] · Jessica Ellen Lima Dias[1]

Accepted: 1 May 2021

Abstract
Damage caused by frost on coffee plants can impact significantly in the reduction of crop quality and productivity. Remote sensing can be used to evaluate the damage caused by frost, providing precise and timely agricultural information to producers, assisting in decision making, and consequently minimizing production losses. In this context, this study aimed to evaluate the potential use of multispectral images obtained by unmanned aerial vehicle (UAV) to analyze and identify damage caused by frost in coffee plants in different climatic favorability zones. Visual evaluations of frost damage and chlorophyll content quantification were carried out in a commercial coffee plantation in Southern Minas Gerais, Brazil. The images were obtained from a multispectral camera coupled to a UAV with rotating wings. The results obtained demonstrated that the vegetation indices had a strong relationship and high accuracy with the frost damage. Among the indices studied the normalized difference vegetation index (NDVI) was the one that had better performances ($r = -0.89$, $R^2 = 0.79$, MAE = 10.87 e RMSE = 14.35). In a simple way, this study demonstrated that multispectral images, obtained from UAV, can provide a fast, continuous, and accessible method to identify and evaluate frost damage in coffee plants. This information is essential for the coffee producer for decision-making and adequate crop management.

Keywords Remote sensing · Vegetation indices · Multispectral images · UAV

Introduction

Coffee is a tropical crop that is currently grown in about 80 countries, being one of the most traded agricultural commodities worldwide. The coffee crop has great importance economically and socially in Brazil which is the world's largest producer and exporter of coffee, but still, a wide number of factors strongly limit agricultural yields and quality of this commodity, including drought and extreme temperatures (Martins et al., 2019).

✉ Diego Bedin Marin
db.marin@hotmail.com

[1] Department of Agricultural Engineering, Federal University of Lavras, P.O BOX 3037, Lavras, MG CEP 37200-000, Brazil

The coffee crop cultivated in regions where air temperature reaches below 18 °C shows a substantially reduced growth index. Besides that, the occurrence of frosting in those regions can limit the economic viability of coffee production (Camargo, 2010). The damage caused by frosting on the coffee plants can cause severe limitations, directly reducing the yield of the year, and impacting in the following years (Ramalho et al., 2014). One of the main effects of frosting in plants is the reduction of the leaf area which can be observed by the reduction of chlorophyll a and b, as well as by the processes of necrosis and senescence of leaves, decreasing the solar radiation absorption and photosynthesis. In this sense, the awareness of the damage caused by frosting is essential for the producer mainly to assist in the decision making to perform, for example, pruning and fertilizing to maintain leaves that were not damaged.

A large part of the national production comes from the southern region of Minas Gerais, an area that has a strong feature on its topography, where high slope and lowlands characterize the geographical relief. In varying terrain, the topography is a known factor that influences the frosting patterns (Kotikot & Onywere, 2014). Therefore, the identification of areas of climate favorability for frost occurrence becomes essential for crop management (Gobbett et al., 2018; Nóia Júnior et al., 2019). Possessing that information, coffee producers could adequately choose the location, orientation, and low-temperature resistant cultivars to be used. Also, for areas showing higher climate risk, especially lowland areas where cold air accumulates, the producer may use preventive measures to reduce the impact of frost on the coffee plants, for example, keep cultivation lines clean from weeds and apply calcium sulcate to increase solute of the plant as well as low-temperature resistance (Camargo, 2010).

To establish a risk zone for frost occurrence is an important step to integrated management and protection of coffee production. Considering the diversity of the geographical reliefs found in coffee-producing areas in Brazil, it is essential to understand how frost formation occurs and how topography influences frost occurrence in coffee plantations. Knowledge of climatic variability affected by topography can help producers identify high and low-risk areas, even when macroclimatic conditions are not favorable.

However, despite the importance of coffee plantations and the occurrence of frost in the producing regions, there are still few studies in the literature evaluating the impact of frost on the coffee crop. Moreover, monitoring damage due to frost requires intensive field survey work (Wei et al., 2017). These procedures, besides being expensive and subjective, are time-consuming and lead to market speculation for coffee, due to the lack of real knowledge of the impact of frost in the region combined with the time to obtain the information (Rafaelli et al., 2006). Thus, it is necessary to develop a more effective approach to define and monitor frost damage for the coffee crop.

Remote sensing can be used to evaluate the damage caused by frost, providing precise and timely agricultural information to producers, assisting in decision making, and consequently minimizing production losses (Marin et al., 2019). The use of remote sensing in agriculture is based on the reflectance characteristics of the leaves in the visible and near-infrared spectral regions, obtained mainly by variations in the photosynthetic pigment content, cell structure, and moisture content (Feng et al., 2018). In the case of frost damage, the reflectance characteristic in the spectral region is modified according to the damage of the cell structure of the leaves (Wang et al., 2015; Wei et al., 2017). Based on that, remote sensing may successfully assess the damage caused by frosting in the coffee crop.

Previous studies have shown potential in orbital remote sensing to monitor damage by plant frosting in different cultures, such as wheat (Feng et al., 2009; Wang et al., 2015), oilseed rape (She et al., 2017; Wei et al., 2017), sugarcane (Tan et al., 2008) and tea (Lou

et al., 2013). For the coffee crop, Rafaelli et al. (2006) reported that normalized difference vegetation index (NDVI), obtained with MODIS images, was enough to monitor the effect of frost in the coffee plantation locally and regionally. However, these studies did not investigate suborbital remote sensing using unmanned aerial vehicle (UAVs) that offers advantages in evaluating injury by frosting when compared to images obtained from satellites. The application of satellite images for evaluation of agricultural cultures might be limited due to the low spatial and temporal resolution, cloudiness, and high operating costs that may not be suitable, especially for smaller farms (Zhang et al., 2016; Zhou et al., 2016). On the other hand, UAVs can collect images with high spatial resolution, down to centimeters, and temporal frequency based on the producer's needs (Zhang et al., 2016). Additionally, it can be used for evaluation in small areas (Santos et al., 2019) with the low-cost advantage in these areas (Zhou et al., 2016).

The lack of information about frost damage in coffee crops grown under different relief conditions limits the ability to understand related plant responses and the economic impacts of this extreme event at a local and regional scale. Therefore, the authors hypothesized that the use of UAVs may contribute to decision-making and adequate management of coffee crops affected by frosting. For this reason, the objective of this study was to evaluate the potential usage of multispectral images obtained by UAV to analyze and identify damage caused by frost in coffee plants in different climatic favorability zones.

Materials and methods

Description of the experimental area

The study was carried out in the coffee farm Bom Jardim, located in the city of Santo Antonio do Amparo, State of Minas Gerais, Brazil, geographical co-ordinates 21°01′11.93″ S, 44°55′24.46″ W and altitude 927 m (Fig. 1). The plantation area represents a total of 3.5 ha cultivating coffee (*Coffea arabica* L.), cultivar Catucaí red IAC 144, aging 6 years old, spaced by 3.5 m between lines and 0.5 m between plants, resulting in 5,700 plants ha^{-1}.

Frost occurrence was observed on July 8th and 9th of 2019. The minimum temperatures on those days were 1.8 and 0.3 °C, respectively. Temperature data were collected from an automatic weather station, located within the coffee farm Bom Jardim. During the winter, the occurrence of extremely low temperatures is a considerable limitation for agriculture, especially for coffee, in the southern region of Minas Gerais. Temperatures there often reach 0 °C, and sometimes, below zero, enabling frost formation and consequently damage to the coffee plants. Furthermore, due to the topographic conditions, frost formation is favored because this region has places with high altitudes and lower flat terrain (lowlands).

Frost risk area classification

To evaluate the effects of frosting in coffee plants, the study area was divided into three distinct areas of climate risk from frost damage. The criteria used were altitude variability and geographical configuration of the terrain. The areas were classified as low, medium, and high climate risk for frost occurrence (Fig. 1). The classification of the study area into three different risk zones was due to the need to understand factors related to climate favorability and to help the coffee producers in decision-making for reducing frost damage before it occurs.

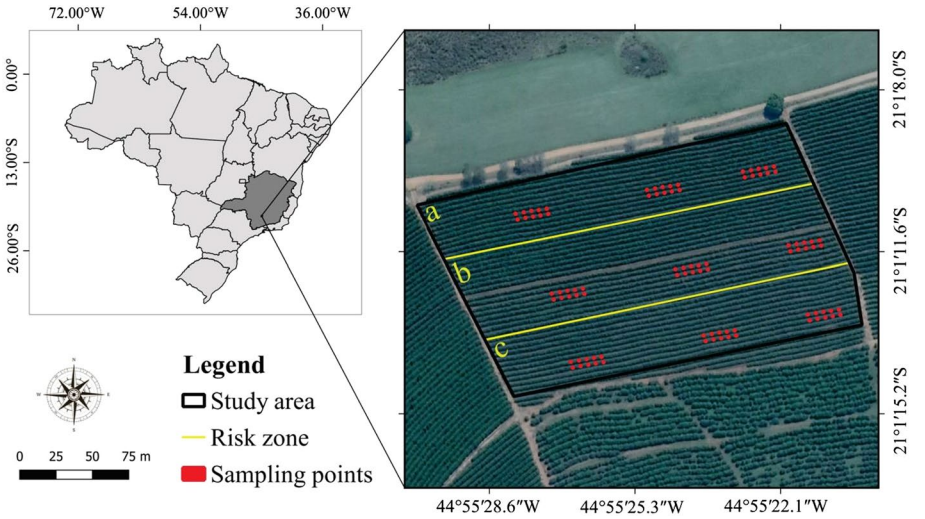

Fig. 1 Geographical location of the study area. The sampling points are highlighted in red points and the climatic favorability zones were separated in yellow lines, where **a** High risk, **b** Medium Risk, and **c** Low risk (Color figure online)

Also, the classification in different risk zones was carried out before the data analysis because the authors aimed to understand and recommend alternatives to reduce possible frost damage. If the coffee producer knows possible plantation areas that present climatic favorability for frost occurrence, he can use strategies to minimize the damage, which would not be possible with the classification of the area after the analysis of the results.

Canopy stratification

The determination of frost damage and chlorophyll content was carried out for each coffee canopy strata. The sampled plants were divided into three canopy sections of similar size to individually analyze the contribution of each canopy strata, according to the location of their vegetative and reproductive structures. The criterion used for sectioning the plant canopy was that to constitute the lower stratum, the plant structures should be located from 0 to 33% of the height of the plants, the middle stratum of 33.34 to 66.66%, and the upper stratum of 66.67 to 100%, respectively.

To analyze the hypothesis that the most significant damage occurred in the upper stratum of the coffee plants, the evaluation of different strata was carried out using vegetation indices obtained by the UAV.

Visual frost damage evaluation

Using a standard scale described in Table 1, based on the percentage of the plant showing frost damage, a visual evaluation was conducted in the coffee plants, including leaves, branches, stem, and fruits on July 11, 2019. The authors considered as frost damage the plant parts that presented brown color and necrosis since that is the aspect caused by cell death by freezing.

Table 1 Classification index and description for assessing frost damage in coffee plants

Damage index	Description
0	No visible damage, %
1	10[a]
2	20
3	30
4	40
5	50
6	60
7	70
8	80
9	90
10	100

[a]% of the plant with visible damage; frost damage in this study was characterized as damage (cell death by necrosis) caused by the effect of frost on the plant parts (leaf, branch, stem, and fruit)

The visual evaluation was carried out in the three different climatic favorability areas and in the different plant strata. To perform the evaluation, three blocks were separated in each climatic favorability area. For each block, 10 plants were selected for evaluation, considering 5 plants of each line. In this context, 30 plants in each risk area were evaluated, resulting in 90 plants data for analysis. The sampling site was chosen, aiming to achieve greater possible representation and homogeneity of the plants in each plot. The location of the selected plants is indicated in Fig. 1.

In this system of evaluation, grades from 0 to 10 were assigned to the different strata of the plant (Table 1). Three experienced observers performed the visual assessment of the frost damage. The end value attributed to the data analysis was the average of the three observer's values.

Evaluation of chlorophyll content

Measurements were made with the atLEAF + chlorophyll meter (FT Green LLC, Wilmington, DE, USA) by clipping the sensor onto the coffee leaf. The measurement area of the sensor atLEAF + was 6 mm^2. All of the measurements were conducted in the morning period, from 9 to 10 am on July 11, 2019, to avoid sunlight interference. In each plant, 15 measurements were conducted, divided into 5 for each stratum. The measurements were conducted in representative leaves of each stratum. To perform the measurement, leaves positioned on the third and fourth pair from the top of the plant were selected. Once the measurement was read, the equations developed and described by Padilha et. al. (2018) were used to estimate the chlorophyll a and chlorophyll b content in mg cm^{-2}.

$$\text{Total Chlorophyll} = 0.078 \times \text{atLEAF}^{1.63} \quad (1)$$

$$\text{Chlorophyll a} = -5.774 + 0.430 \times \text{atLEAF} + 0.0045 \times \text{atLEAF}^2 \quad (2)$$

$$\text{Chlorophyll b} = 0.040 \times \text{atLEAF}^{1.57} \quad (3)$$

where atLEAF is the value measured by the sensor.

Acquisition of multispectral images

The commercial UAV 3DR Solo (3D Robotics, Berkeley, CA, USA) was used to collect the multispectral images on July 11, 2019, 2 days after the frost occurrence. The UAV had rotating wings and four motors (quadcopter), driven by the automatic pilot system 3DR Pixhawk 2, and flight controller APM: Copter (Duffy et al., 2018) (Fig. 2a). The UAV was equipped with a multispectral camera Parrot Sequoia (MicaSense, Seattle, WA, USA) (Fig. 2b), comprising four spectral sensors, 1.5 megapixels resolution (1280×960), spectral bands of green (530–570 nm), red (640–680 nm), red-edge (730–740 nm) and near-infrared (770–810 nm). This camera was used to map and monitor vegetation. It includes a sunshine sensor (Fig. 2c) pointing upwards, that allowed radiometric calibration during image collection (MicaSense Sequoia, 2018). Additionally, to transform digital numbers (gray levels) from sensors to reflectance values, a calibrated reflectance panel (MicaSense, Seattle, WA, USA) (Fig. 2d) was used before and after the flight (Freitas et al., 2019).

The 3DR Solo is capable of performing flights being remotely controlled or autonomously while using a global navigation satellite system (GNSS) and a navigation system by waypoint. For this study, the flights were operated autonomously. The flight missions were planned using the Mission Planner (Oborne, 2018), a complete and open source ground station software for UAV autopilot systems (Lu et al., 2016), running on a portable computer. The flight altitude was fixed at 60 m from the ground, and the speed was 3 m s^{-1}.

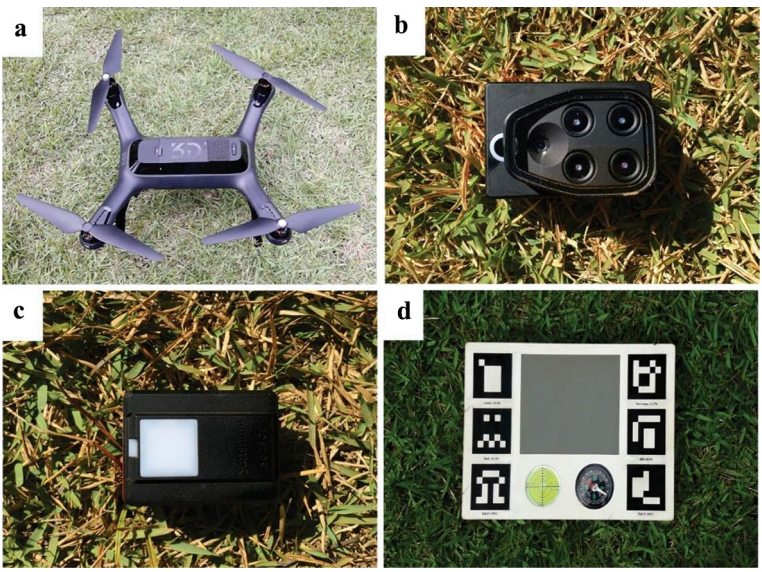

Fig. 2 **a** UAV 3DR Solo; **b** Multispectral Parrot Sequoia camera; **c** Sunshine sensor; **d** Calibrated reflectance panel

The images were captured at every 1 s, with a frontal and lateral overlap of 80%, resulting in a total of 150 images with a spatial resolution of 64.4 mm.

Image processing

The image processing was performed by the software Pix4Dmapper, version 4.4.12 (Pix4D, Lausanne, Switzerland). This software contains computational vision technics that allow photogrammetry algorithms that obtain high precision processing in aerial images (Ruzgienė et al., 2015). The standard template "Ag Multispectral" from Pix4Dmapper was used to generate the orthomosaics from individual spectral bands (green, red, red-edge, and near-infrared). To improve the precision and the accuracy of the orthomosaics, the images were georeferenced using control points collected previously in the field area by a differential GNSS (Trimble Navigation Limited, Sunnyvale, California, USA) spectra precision model SP 60 with a horizontal and vertical accuracy of 0.07 m. Additionally, the calibrated reflectance panel corrected the reflectance of the images. After generating the orthomosaics, the vegetation indices were calculated using the Pix4D and exported to the TIFF extension for later analysis. For that, the average value extracted from the pixels in a 0.20 m radius was calculated from the center of each plant sampled, using the Zonal Statistics resource available on the QGIS 2.18.13 (QGIS Development Team, 2017).

Vegetation indices

Based on the literature, there are no studies applying vegetation indices to evaluate the damage caused by frost in coffee plants. However, for choosing vegetation indices, a literature revision was made to identify the indices capable of differentiating characteristics from stress conditions in coffee plants, and with the capacity to evaluate the spectral response of the plants due to frost damage. After this revision, the vegetation indices chosen were the ones that had two characteristics at the same time, that is the capacity to assess the stress conditions of the coffee plants and the spectral response of the plants after frost damage (Table 2).

Statistical analysis

The statistical analysis was performed on the software R version 3.4 (R Core Team 2017). The significant differences in the frost damage analysis and the chlorophyll content in the climatic favorability zones were measured by the Tukey test ($p < 0.05$). To evaluate the linear relation between the vegetation indices and the occurrence of frost in the upper stratum of the plants, and in the whole plant, the respective data sets were subjected to Pearson's correlation (r) analysis ($p < 0{,}01$) and coefficient of determination (R^2). The average values for vegetation indices were obtained from the present pixels in a 0.20 m radius from the center of each plant.

To value the performance of the vegetation indices on the estimation of the damage caused by frost in coffee plants, the following statistical indices were applied: mean absolute error (MAE) (Eq. 4), root mean square error (RMSE) (Eq. 5), and index of agreement (d) (Eq. 6).

Table 2 Vegetation indices of multispectral images obtained using UAV

Vegetation indices	Calculation	References
NDVI (normalized difference vegetation index)	$\frac{\rho_{nir}-\rho_{red}}{\rho_{nir}+\rho_{red}}$	Rouse et al. (1974)
MSR (modified simple ratio)	$\frac{\left(\frac{\rho_{nir}}{\rho_{red}}\right)-1}{\sqrt{\left(\frac{\rho_{nir}}{\rho_{red}}\right)+1}}$	Chen (1996)
SAVI (soil adjusted difference vegetation index)	$\frac{(1+L)\rho_{nir}-\rho_{red}}{\rho_{nir}+\rho_{red}+L}$	Huete (1988)
GNDVI (green normalized difference vegetation index)	$\frac{\rho_{nir}-\rho_{green}}{\rho_{nir}+\rho_{green}}$	Gitelson et al. (1996)
MTCI (terrestrial chlorophyll index)	$\frac{\rho_{nir}-\rho_{edge}}{\rho_{edge}+\rho_{red}}$	Dash and Curran (2004)
NDRE (normalized difference red edge)	$\frac{\rho_{nir}-\rho_{edge}}{\rho_{nir}+\rho_{edge}}$	Gitelson and Merzlyak (1994)
NDI (normalized different index)	$\frac{\rho_{green}-\rho_{red}}{\rho_{green}+\rho_{red}+0.01}$	Mao et al. (2003)
MPRI (modified photochemical reflectance index)	$\frac{\rho_{green}-\rho_{red}}{\rho_{green}+\rho_{red}}$	Yang et al. (2008)
MCARI1 (first modified chlorophyll absorption ratio index)	$1.2[2.5(\rho_{nir}-\rho_{red})-1.3((\rho_{nir}-\rho_{green})]$	Haboudane et al. (2004)

ρ_{green}: green band reflectance; ρ_{red}: red band reflectance; ρ_{edge}: red-edge band reflectance; ρ_{nir}: near-infrared band reflectance

$$MAE = \frac{1}{n}\sum_{i=1}^{n}\left|P_i - O_i\right| \tag{4}$$

$$RMSE = \sqrt{\frac{1}{n}\sum_{i=1}^{n}\left(P_i - O_i\right)^2} \tag{5}$$

$$d = 1 - \left[\frac{\sum_{i=1}^{n}\left(P_i - O_i\right)^2}{\sum_{i=1}^{n}\left(\left|P'_i\right| + \left|O'_i\right|\right)^2}\right] \tag{6}$$

where, n is the number of observations, P_i the predicted observation based on the linear regression model, O_i is a measured observation, $P'_i = P_i - M$ and $O'_i = O_i - M$ (M is the mean of the observed variable).

Results and discussion

Frost damage in different coffee canopy strata

The coffee plants evaluated in the low climate risk areas did not show frost damage for any stratum of the plant (Table 3). This indicates a significant interference of the topography in the favorability for frost occurrence since, in the other evaluated areas, the effect of frost was observed, mainly in the upper stratum of the plants.

Table 3 Frost damage (FD) and standard deviation (SD) in different coffee canopy strata and whole plant at different climatic favorability zones in the area studied

Coffee canopy	Climatic favorability zones					
	Low		Average		High	
	FD (%)	SD	FD (%)	SD	FD (%)	SD
Lower	0 b*	±0	3 b	±0.29	14 a	±2.25
Middle	0 c	±0	11 b	±1.74	43 a	±4.92
Upper	0 c	±0	30 b	±5.8	78 a	±8.45
Whole plant	0 c	–	15 b	–	45 a	–

*Different small letters indicate significant differences ($p < 0.05$) by Tukey test among climatic favorability zones for each coffee canopy strata and whole plant

Significant differences for frost damage in coffee plants were observed among the climatic risk zones. The higher frost damage value was observed in the upper canopy stratum that was located in the high climate risk zone for frost occurrence. The coffee evaluated in the average climate risk zone showed higher values than the low climatic risk for the middle and upper canopy stratum. When combined with the whole plant, the average damage caused by frost in the areas of high, medium, and lower climatic favorability was 45, 15, and 0% respectively.

The frost damage in the upper stratum of the plant can have a significant effect on the coffee production, reducing the leaf area and, consequently, the photosynthetic activity, compromising the accumulation of dry matter, decreasing productivity in the current harvest and during the next cycles of the crop (DaMatta & Ramalho, 2006).

Being aware of the damage caused by frost is essential for coffee producers to assist in decision-making and agricultural planning. For example, in the high climatic risk areas, plants have shown 45% of the leaf area damaged. In this case, the producer could decide to perform a drastic pruning on the plants. Also, according to the results of this study, the most damaged area in the plant was the upper stratum. In this case, the producer could perform the pruning only in that region of the plant, exposing the less damaged leaves.

The establishment of risk zones for frost occurrence and coffee leaf damage is an important step towards an integrated management plan for these events. The identification and classification of zones of greater or lesser climatic favorability are important for the coffee producers, for them to perform appropriate management in the production area, considering, for example, the topography and the areas where cold air accumulates. Because of the effects of land surface heterogeneity on spatial variation of near-surface temperatures, the spatial occurrence of frost can be linked to land surface characteristics (Kotikot et al., 2020). Of most importance is the concept of cold air pooling where cold dense air flows downslope and settles beneath warmer air (Kotikot et al., 2020). For this reason, low temperatures and therefore frost zones tend to accumulate in low regions of the landscape (Bigg et al., 2014; Chung et al., 2006). In this context, the information generated in this study can help coffee producers to avoid the use of susceptible cultivars in those zones where frost occurrence poses the greatest risk, and to optimize strategies for reducing the damage by frost in coffee plants.

When analyzing the chlorophyll content in the different canopy strata and climatic risk zones (Table 4), it is possible to observe a little variation in the chlorophyll a, b,

Table 4 Chlorophyll index (a, b, and total) and standard deviation (SD) in different coffee canopy strata and whole plant at different climatic favorability zones in the studied area

Coffee canopy	Climatic favorability zones					
	Low		Average		High	
	Chlorophyll a					
	CA (μg cm^{-2})	SD	CA (μg cm^{-2})	SD	CA (μg cm^{-2})	SD
Lower	39.48 a*	±1.4	36.69 a	±1.9	40.21 a	±0.6
Middle	40.16 a	±2.4	37.73 a	±3.3	36.17 b	±0.5
Upper	46.41 a	±2.7	32.8 b	±5.1	21.39 c	±1.4
Whole plant	42.02 a	±1.5	35.74 b	±3.4	32.59 b	±0.5
Coffee canopy	Chlorophyll b					
	CB (μg cm^{-2})	SD	CB (μg cm^{-2})	SD	CB (μg cm^{-2})	SD
Lower	26.93 a	±0.9	25.07 a	±1.3	27.42 a	±0.4
Middle	27.39 a	±1.8	25.77 a	±2.2	24.72 a	±0.3
Upper	31.56 a	±1.6	22.48 b	±3.4	14.91 c	±0.9
Whole plant	28.63 a	±1.1	24.44 ab	±2.3	22.35 b	±0.3
Coffee canopy	Total Chlorophyll					
	CT (μg cm^{-2})	SD	CT (μg cm^{-2})	SD	CT (μg cm^{-2})	SD
Lower	66.41 a	±2.3	61.76 a	±2.2	67.63 a	±1.0
Middle	67.55 a	±4.0	63.5 ab	±5.5	60.89 b	±0.8
Upper	77.98 a	±4.3	55.28 b	±8.5	36.3 c	±2.3
Whole plant	70.65 a	±2.7	60.18 b	±5.7	54.94 c	±0.8

*Different small letters indicate significant differences ($p < 0.05$) by Tukey test among climatic favorability zones for each coffee canopy strata and whole plant

and total content for middle and lower strata, regardless of the climate risk zone. However, for the upper stratum of the coffee plants, the content of chlorophyll a, b, and total were higher for the area of lower climate risk. Considering the total value of chlorophyll (a + b), a significant reduction in the medium and high-risk zones was observed when comparing it to the low-risk zone of climate favorability.

The response observed in the chlorophyll content follows the same pattern seen in the results reported on frost damage, shown in Table 3, where the upper stratum has presented greater frost damage and lower chlorophyll content. It is important to highlight that the reduction in the chlorophyll content of coffee leaves is due to the damage caused by frosting. In cases of extreme temperatures, such as frost occurrence, the degradation of chlorophyll is associated with the structural changes that release cellular acids and various degradative enzymes (Hodges & Forney, 2000). Therefore, the reduction of the chlorophyll content in coffee plants due to frosting, mainly in the upper stratum, significantly impacts the photosynthetic efficiency, and in the productivity of the plant. In this sense, the two variables are associated, being the visual damage observed and reduction of the chlorophyll content.

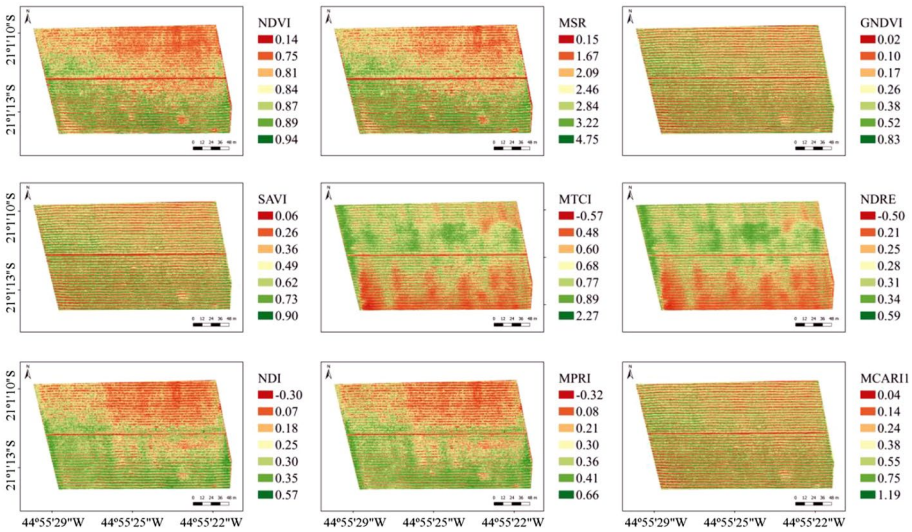

Fig. 3 Spatial distribution of vegetation indices in the study area

Spatial distribution of vegetation indices

The spatial distribution of the vegetation indices in the study area can be seen in Fig. 3. The maps of NDVI, MSR, NDI, and MPRI have shown the lower values in the high climatic favorability area of the crop, and the greater values in low-risk areas, evidencing the effect of relief in the frost occurrence. According to Caramori et al. (2001), the crops located in lowlands and terrains with concave configuration and small slopes have a higher probability of frost occurrence. As for the indices GNDVI, SAVI, MTCI, NDRE, and MCARI1, the spatial distribution made it difficult to identify and map the effect of frost in the coffee plants.

Knowledge of the characteristics and spatial distribution of the frosting effect on the coffee crop is highly applicable in the orientation of extension workers in the field, governmental agencies, and agricultural producers to support decision-making regarding the management of the coffee crop. This is more emphasized by the fact that one of the effects of frosting in coffee plants is a reduction in the productivity of the crop (Carvalho et al., 2017). Therefore, the vegetation indices can quickly, precisely, and continuously indicate areas of the crop that need lighter or drastic pruning, or even dispense with pruning. Besides that, in severe cases, it can be a useful tool to assist the application of agricultural insurance to compensate for losses. In this context, Rafaelli et al. (2006) have successfully demonstrated the potential of the NDVI index, obtained with MODIS sensor images, for monitoring coffee crops affected by frosting at a state scale, for the state of Paraná, in the South of Brazil.

However, orbital sensors like MODIS show limitations that make it difficult to monitor and evaluate the frosting effect continuously at local scales. Those limitations include low spatial resolution (250–500 m) that can be influenced by other spectral targets compromising its accuracy (Feng et al., 2017; Ke et al., 2016). A potential solution for this problem is high spatial resolution satellites, even though, the acquisition of data from them is expensive and limited due to cloudiness (Hellweger et al., 2007; Müllerová et al., 2017), which

is not ideal for analyzing the effect of frost in coffee plants. When working with vegetation indices obtained from UAVs, those limitations are reduced, since the images can be captured continuously and with high spatial resolution, decreasing the interference of other spectral targets present in the crop.

Evaluation of the estimation of frost damage generated by vegetation indices

The results of the performance evaluation of the vegetation indices on estimating the frost damage in the upper stratum of coffee plants are shown in Table 5. It was possible to observe that the occurrence of frost in the upper stratum and the whole plant presented similar correlation coefficients with the vegetation indices, validating the hypothesis that the evaluation of the upper stratum is enough to measure the frost damage when using images captured by UAVs.

The correlation coefficients (r) and the determination coefficients (R^2) have shown strong relationships to vegetation indices and frost damage. Regarding the accuracy, most of the vegetation indices have presented MAE and RMSE values between 10 to 20%, evidencing the potential of the vegetation indices in evaluating damage by frost. According to Jamieson et al. (1991), the model is considered excellent if the normalized RMSE is inferior to 10%, good if the normalized RMSE is between 10 and 20%, fair if the normalized RMSE is greater than 20 but inferior to 30%, and bad if the normalized RMSE is greater than 30%. Besides that, the values of the index of agreement (d) between 0.73 to 0.89

Table 5 Statistics indices between frost damage and vegetation indices

Vegetation Indice	MAE[a]	RMSE	d	R^2	r
Whole plant					
NDVI	13.66	16.72	0.87	0.72	−0.85
MSR	14.01	16.99	0.86	0.69	−0.83
GNDVI	21.21	25.99	0.79	0.38	−0.62
SAVI	19.88	23.51	0.81	0.42	−0.65
MTCI	27.99	31.54	0.73	0.20	0.45
NDRE	28.09	32.11	0.73	0.19	0.44
NDI	14.13	17.08	0.85	0.66	−0.81
MPRI	14.14	17.10	0.85	0.66	−0.81
MCARI1	23.57	27.77	0.77	0.29	−0.54
Upper stratum					
NDVI	10.87	14.35	0.89	0.79	−0.89
MSR	11.01	14.70	0.88	0.77	−0.88
GNDVI	19.92	23.67	0.82	0.46	−0.68
SAVI	17.45	21.89	0.83	0.55	−0.74
MTCI	25.31	28.84	0.76	0.26	0.51
NDRE	27.93	31.50	0.73	0.20	0.45
NDI	13.95	16.92	0.86	0.69	−0.83
MPRI	13.88	16.82	0.87	0.70	−0.84
MCARI1	25.36	28.80	0.76	0.26	−0.51

[a]Statistics indices: MAE (mean absolute error), RMSE (root mean square error), d (index of agreement), R^2 (determination coefficient), and r (correlation coefficient)

confirm the quality of the model, because the (d) represents the ratio between the squared average error and the potential error, where the concordance value equals 1 indicates the perfect combination (Willmott, 1981).

In general, the vegetation indices NDVI and MSR, which are indices that use the combination of near-infrared reflectance with the red reflectance, showed better performance in estimating the damage caused by frost in coffee plants. On the other hand, the indices GNDVI, SAVI, MTCI, and NDRE, which combine the near-infrared reflectance with the green and red-edge reflectance, showed the worst performance. The NDI and MPRI indices that use reflectance of the green and red wavelengths, showed performance close to the best ones (NDVI and MSI), demonstrating that the visible spectral region is directly related to the frost damage in the coffee plants.

The best performance for indices that used the red wavelength can be associated with the color change in the leaves due to the frosting. According to Larcher (1981), frost causes the death of vegetation tissue by a physical–chemical process. The results of these processes are dehydration of the cell, loss of turgor potential, increase of solute concentration, reduction of cellular volume, and rupture of the plasmatic membrane. Thus, the leaves become dark brown colored, with a burning aspect.

Although these indices presented the best performance, better results were expected for indices that use green and red-edge wavelengths, since these wavelengths are directly related to the chlorophyll content in leaves damaged by frosting (Table 4). This relationship is in line with other studies that have shown that the chlorophyll content is significantly correlated to the green and red-edge wavelengths (Devadas et al., 2009; Li et al., 2007).

It is worth mentioning that the NDI and MPRI are indices that use only visible wavelengths, showed elevated performance and results, close to the vegetation indices with the best results (NDVI and MSR). Because of that, RGB cameras have become an interesting alternative for producers, being easier to operate and lower cost compared to multispectral cameras. They also require little data processing and present reliable results (Barbosa et al., 2019; Svensgaard et al., 2019). As in this study, Nuttall et al. (2019) also observed that RGB vegetation indices are reliable in evaluating the damage caused by frost. However, NDVI still stands as more efficient to map, monitor, and identify damage in plants provoked by frosting (Feng et al., 2009; Rafaelli et al., 2006; Wei et al., 2017).

Conclusion

The multispectral images obtained using UAV can provide for the coffee producers a fast, continuous and accessible method to identify and evaluate frost damage in coffee plants, confirming the hypothesis of this study. Specifically, the NDVI and MSR (indices that use the combination of near-infrared and red spectral bands) have shown better results. Otherwise, the indices MTCI and NDRE which use the red-edge band showed the worst results. The spatial distribution of the vegetation indices indicated that the topography is directly related to the frost occurrence in the coffee plantation. Greatest damage and lower chlorophyll a and b content were observed in areas with greater climatic risk (lowlands) for the upper strata of the plant.

Due to climate change and its consequences, extreme events are becoming more frequent, making it even more essential to comprehend the physiological response of coffee plants after frosting. Therefore, other research using UAVs with greater autonomy and other sensors can contribute even more to the understanding of this relationship, as well as assisting producers on how to manage their crops.

Acknowledgements This work was supported by the Embrapa Café—Consórcio Pesquisa Café, project approved in the call n° 20/2018, the National Council for Scientific and Technological Development (CNPq), the Coordination for the Improvement of Higher Education Personnel (CAPES), the Federal University of Lavras (UFLA) and farm Bom Jardim.

Declarations

Conflict of interest The authors declare that they have no conflict of interest.

References

Barbosa, B. D. S., Ferraz, G. A. S., Santos, L. M., Marin, D. B., Maciel, D. T., Ferraz, P. F. P., & Rossi, G. (2019). RGB vegetation indices applied to grass monitoring: A qualitative analysis. *Agronomy Research, 17*(2), 349–357

Bigg, G. R., Wise, S. M., Hanna, E., Mansell, D., Bryant, R. G., & Howard, A. (2014). Synoptic climatology of cold air drainage in the Derwent Valley, Peak District, UK. *Meteorological Applications, 21*(2), 161–170. https://doi.org/10.1002/met.1317

Camargo, M. B. P. D. (2010). The impact of climatic variability and climate change on Arabic coffee crop in Brazil. *Bragantia, 69*(1), 239–247. https://doi.org/10.1590/S0006-87052010000100030

Caramori, P. H., Caviglione, J. H., Wrege, M. S., Gonçalves, S. L., Faria, R. T., Filho, A. A., Sera, T., Chaves, J. C. D., & Koguishi, M. S. (2001). Climatic risk zoning for coffee (*Coffea arabica* L.) in Paraná state, Brazil. *Revista Brasileira de Agrometeorologia*, 9(3), 486–494.

Carvalho, L. C., Silva, F. M. D., Ferraz, G. A., Stracieri, J., Ferraz, P. F., & Ambrosano, L. (2017). Geostatistical analysis of Arabic coffee yield in two crop seasons. *Revista Brasileira De Engenharia Agrícola e Ambiental, 21*(6), 410–414. https://doi.org/10.1590/1807-1929/agriambi.v21n6p410-414

Chen, J. M. (1996). Evaluation of vegetation indices and a modified simple ratio for boreal applications. *Canadian Journal of Remote Sensing, 22*(3), 229–242. https://doi.org/10.1080/07038992.1996.10855178

Chung, U., Seo, H. H., Hwang, K. H., Hwang, B. S., Choi, J., Lee, J. T., & Yun, J. I. (2006). Minimum temperature mapping over complex terrain by estimating cold air accumulation potential. *Agricultural and Forest Meteorology, 137*(1–2), 15–24. https://doi.org/10.1016/j.agrformet.2005.12.011

DaMatta, F. M., & Ramalho, J. D. C. (2006). Impacts of drought and temperature stress on coffee physiology and production: A review. *Brazilian Journal of Plant Physiology, 18*(1), 55–81. https://doi.org/10.1590/S1677-04202006000100006

Dash, J., & Curran, P. J. (2004). The MERIS terrestrial chlorophyll index. *International Journal of Remote Sensing, 25*(23), 5403–5413. https://doi.org/10.1080/0143116042000274015

Devadas, R., Lamb, D. W., Simpfendorfer, S., & Backhouse, D. (2009). Evaluating ten spectral vegetation indices for identifying rust infection in individual wheat leaves. *Precision Agriculture, 10*(6), 459–470. https://doi.org/10.1007/s11119-008-9100-2

Duffy, J. P., Pratt, L., Anderson, K., Land, P. E., & Shutler, J. D. (2018). Spatial assessment of intertidal seagrass meadows using optical imaging systems and a lightweight drone. *Estuarine, Coastal and Shelf Science, 200*, 169–180. https://doi.org/10.1016/j.ecss.2017.11.001

Feng, G., Anderson, M. C., Zhang, X., Yang, Z., Alfieri, J. G., Kustas, W. P., Mueller, R., Johnson, D. M., & Prueger, J. H. (2017). Toward mapping crop progress at field scales through fusion of Landsat and MODIS imagery. *Remote Sensing of Environment, 188*, 9–25. https://doi.org/10.1016/j.rse.2016.11.004

Feng, M., Guo, X., Wang, C., Yang, W., Shi, C., Ding, G., Zhang, X., Xiao, L., Zhang, M., & Song, X. (2018). Monitoring and evaluation in freeze stress of winter wheat (*Triticum aestivum* L.) through canopy hyperspectrum reflectance and multiple statistical analysis. *Ecological Indicators, 84*, 290–297. https://doi.org/10.1016/j.ecolind.2017.08.059

Feng, M. C., Yang, W. D., Cao, L. L., & Ding, G. W. (2009). Monitoring winter wheat freeze injury using multi-temporal MODIS data. *Agricultural Sciences in China, 8*(9), 1053–1062. https://doi.org/10.1016/S1671-2927(08)60313-2

Freitas, P., Vieira, G., Canário, J., Folhas, D., & Vincent, W. F. (2019). Identification of a threshold minimum area for reflectance retrieval from thermokarst lakes and ponds using full-pixel data from Sentinel-2. *Remote Sensing, 11*(6), 657. https://doi.org/10.3390/rs11060657

Gitelson, A. A., Kaufman, Y. J., & Merzlyak, M. N. (1996). Use of a green channel in remote sensing of global vegetation from EOS-MODIS. *Remote Sensing of Environment, 58*(3), 289–298. https://doi.org/10.1016/S0034-4257(96)00072-7

Gitelson, A., & Merzlyak, M. N. (1994). Quantitative estimation of chlorophyll-a using reflectance spectra: Experiments with autumn chestnut and maple leaves. *Journal of Photochemistry and Photobiology b: Biology, 22*(3), 247–252. https://doi.org/10.1016/1011-1344(93)06963-4

Gobbett, D. L., Nidumolu, U., & Crimp, S. (2018). Modelling frost generates insights for managing risk of minimum temperature extremes. *Weather and Climate Extremes, 27*, 100176. https://doi.org/10.1016/j.wace.2018.06.003

Haboudane, D., Miller, J. R., Pattey, E., Zarco-Tejada, P. J., & Strachan, I. B. (2004). Hyperspectral vegetation indices and novel algorithms for predicting green LAI of crop canopies: Modeling and validation in the context of precision agriculture. *Remote Sensing of Environment, 90*(3), 337–352. https://doi.org/10.1016/j.rse.2003.12.013

Hellweger, F. L., Miller, W., & Oshodi, K. S. (2007). Mapping turbidity in the Charles River, Boston using a high-resolution satellite. *Environmental Monitoring and Assessment, 132*(1–3), 311–320. https://doi.org/10.1007/s10661-006-9535-8

Hodges, D. M., & Forney, C. F. (2000). The effects of ethylene, depressed oxygen and elevated carbon dioxide on antioxidant profiles of senescing spinach leaves. *Journal of Experimental Botany, 51*(344), 645–655. https://doi.org/10.1093/jexbot/51.344.645

Huete, A. R. (1988). A soil-adjusted vegetation index (SAVI). *Remote Sensing of Environment, 25*(3), 295–309. https://doi.org/10.1016/0034-4257(88)90106-X

Jamieson, P. D., Porter, J. R., & Wilson, D. R. (1991). A test of the computer simulation model ARCWHEAT1 on wheat crops grown in New Zealand. *Field Crops Research, 27*(4), 337–350. https://doi.org/10.1016/0378-4290(91)90040-3

Ke, Y., Im, J., Park, S., & Gong, H. (2016). Downscaling of MODIS One kilometer evapotranspiration using Landsat-8 data and machine learning approaches. *Remote Sensing, 8*(3), 215. https://doi.org/10.3390/rs8030215

Kotikot, S. M., Flores, A., Griffin, R. E., Nyaga, J., Case, J. L., Mugo, R., Sedah, A., Adams, E., Limaye, A., & Irwin, D. E. (2020). Statistical characterization of frost zones: Case of tea freeze damage in the Kenyan highlands. *International Journal of Applied Earth Observation and Geoinformation, 84*, 101971. https://doi.org/10.1016/j.jag.2019.101971

Kotikot, S. M., & Onywere, S. M. (2014). Application of GIS and remote sensing techniques in frost risk mapping for mitigating agricultural losses in the Aberdare ecosystem, Kenya. *Geocarto International, 30*, 104–121. https://doi.org/10.1080/10106049.2014.965758

Larcher, W. (1981). Effects of low temperature stress and frost injury on plant productivity. In C. B. Johnson (Ed.), *Physiological processes limiting plant productivity.* (pp. 253–269). London, UK: Butterworths.

Li, X. Y., Liu, G. S., Yang, Y. F., Zhao, C. H., Yu, Q. W., & Song, S. X. (2007). Relationship between hyperspectral parameters and physiological and biochemical indexes of flue-cured tobacco leaves. *Agricultural Sciences in China, 6*(6), 665–672. https://doi.org/10.1016/S1671-2927(07)60098-4

Lou, W., Ji, Z., Sun, K., & Zhou, J. (2013). Application of remote sensing and GIS for assessing economic loss caused by frost damage to tea plantations. *Precision Agriculture, 14*(6), 606–620. https://doi.org/10.1007/s11119-013-9318-5

Lu, B., He, Y., & Liu, H. (2016). Investigating species composition in a temperate grassland using Unmanned Aerial Vehicle-acquired imagery. In 2016 4th international workshop on earth observation and remote sensing applications (EORSA). IEEE, (pp. 107–111). https://doi.org/10.1109/EORSA.2016.7552776.

Mao, W., Wang, Y., & Wang, Y. (2003). Real-time detection of between-row weeds using machine vision. Paper No. 031004, St Joseph, MI, USA: ASAE. https://doi.org/10.13031/2013.15381.

Marin, D. B., Alves, M. C., Pozza, E. A., Gandia, R. M., Cortez, M. L. J., & Mattioli, M. C. (2019). Multispectral remote sensing in the identification and mapping of biotic and abiotic coffee tree variables. *Revista Ceres, 66*(2), 142–153. https://doi.org/10.1590/0034-737x201966020009

Martins, M. Q., Partelli, F. L., Golynski, A., Sousa Pimentel, N., Ferreira, A., de Oliveira Bernardes, C., Ribeiro-Barros, A. I., & Ramalho, J. C. (2019). Adaptability and stability of Coffea canephora genotypes cultivated at high altitude and subjected to low temperature during the winter. *Scientia Horticulturae, 252*, 238–242. https://doi.org/10.1016/j.scienta.2019.03.044

MicaSense Sequoia. (2018). Sequoia User Guide. Drones Parrot SAS, (pp. 4–13). Paris, France. Retrieved 30 Mar, 2021 from www.micasense.com/sequoia.

Müllerová, J., Brůna, J., Bartaloš, T., Dvořák, P., Vítková, M., & Pyšek, P. (2017). Timing is important: unmanned aircraft vs. satellite imagery in plant invasion monitoring. *Frontiers in Plant Science, 8*, 887. https://doi.org/10.3389/fpls.2017.00887

Nóia Júnior, R. N., Schwerz, F., Safanelli, J. L., Rodrigues, J. C., & Sentelhas, P. C. (2019). Eucalyptus rust climatic risk as affected by topography and ENSO phenomenon. *Australasian Plant Pathology, 48*(2), 131–141. https://doi.org/10.1007/s13313-018-0608-2

Nuttall, J. G., Perry, E. M., Delahunty, A. J., O'Leary, G. J., Barlow, K. M., & Wallace, A. J. (2019). Frost response in wheat and early detection using proximal sensors. *Journal of Agronomy and Crop Science, 205*(2), 220–234. https://doi.org/10.1111/jac.12319

Padilla, F. M., Souza, R., Peña, T., Gallardo, M., Gimenez, C., & Thompson, R. (2018). Different responses of various chlorophyll meters to increasing nitrogen supply in sweet pepper. *Frontiers in Plant Science, 9*, 1752. https://doi.org/10.3389/fpls.2018.01752

Oborne, M. (2018). Mission Planner. Retrieved 30 Mar, 2021 from https://ardupilot.org/planner/index.html

QGIS Development Team. (2017). QGIS geographic information system. Open Source Geospatial Foundation Project. Retrieved 30 Mar, 2021 from http://www.qgis.org

R Development Core Team. (2017). R: A language and environment for statistical computing. R Foundation for Statistical Computing, Vienna, Austria.

Rafaelli, D. R., Moreira, M. A., & Farias, R. (2006). Analysis of the MODIS data potential to monitor (state and local level) frost impact on coffee. *Agricultura Em São Paulo, 53*(1), 5–15

Ramalho, J. C., DaMatta, F. M., Rodrigues, A. P., Scotti-Campos, P., Pais, I., Batista-Santos, P., Partelli, F. L., Ribeiro, A., Lidon, F. C., & Leitão, A. E. (2014). Cold impact and acclimation response of *Coffea* spp. plants. *Theoretical and Experimental Plant Physiology, 26*(1), 5–18. https://doi.org/10.1007/s40626-014-0001-7

Rouse, J. W., Haas, R. H., Deering, D. W., Schell, J. A., & Harlan, J. C. (1974). Monitoring the Vernal Advancement and Retrogradation (Green Wave Effect) of Natural Vegetation. Greenbelt: NASA/GSFC, Type III, Final Report, 371p.

Ruzgienė, B., Berteška, T., Gečyte, S., Jakubauskienė, E., & Aksamitauskas, V. Č. (2015). The surface modelling based on UAV Photogrammetry and qualitative estimation. *Measurement, 73*, 619–627. https://doi.org/10.1016/j.measurement.2015.04.018

Santos, L. M. D., Andrade, M. T., Santana, L. S., Rossi, G., Maciel, D. T., Barbosa, B. D. S., Maciel, D. T., & Rossi, G. (2019). Analysis of flight parameters and georeferencing of images with different control points obtained by RPA. *Agronomy Research, 17*(5), 2054–2063

She, B., Huang, J. F., Zhang, D. Y., & Huang, L. S. (2017). Assessing and characterizing oilseed rape freezing injury based on MODIS and MERIS data. *International Journal of Agricultural and Biological Engineering, 10*(3), 143–157

Svensgaard, J., Jensen, S. M., Westergaard, J. C., Nielsen, J., Christensen, S., & Rasmussen, J. (2019). Can reproducible comparisons of cereal genotypes be generated in field experiments based on UAV imagery using RGB cameras? *European Journal of Agronomy, 106*, 49–57. https://doi.org/10.1016/j.eja.2019.03.006

Tan, Z., Ding, M., Wang, L., Yang, X., & Ou, Z. (2008). Monitoring freeze injury and evaluating losing to sugarcane using RS and GPS. In *International Conference on Computer and Computing Technologies in Agriculture* (pp. 307–316). Boston, USA: Springer.

Wang, H., Huo, Z., Zhou, G., Wu, L., & Feng, H. (2015). Monitoring and forecasting winter wheat freeze injury and yield from multi-temporal remotely sensed data. *Intelligent Automation & Soft Computing, 22*(2), 255–260. https://doi.org/10.1080/10798587.2015.1095475

Wei, C., Huang, J., Wang, X., Blackburn, G. A., Zhang, Y., Wang, S., & Mansaray, L. R. (2017). Hyperspectral characterization of freezing injury and its biochemical impacts in oilseed rape leaves. *Remote Sensing of Environment, 195*, 56–66. https://doi.org/10.1016/j.rse.2017.03.042

Willmott, C. J. (1981). On the validation of models. *Physical Geography, 2*(2), 184–194. https://doi.org/10.1080/02723646.1981.10642213

Yang, Z., Willis, P., & Mueller, R. (2008). Impact of band-ratio enhanced AWIFS image to crop classification accuracy. In *Proceedings of the 17th william pecora memorial remote* sensing symposium, (pp. 1–11). Bethesday, MD, USA: American Society for Photogrammetry & Remote Sensing.

Zhang, J., Hu, J., Lian, J., Fan, Z., Ouyang, X., & Ye, W. (2016). Seeing the forest from drones: Testing the potential of lightweight drones as a tool for long-term forest monitoring. *Biological Conservation, 198*, 60–69. https://doi.org/10.1016/j.biocon.2016.03.027

Zhou, J., Pavek, M. J., Shelton, S. C., Holden, Z. J., & Sankaran, S. (2016). Aerial multispectral imaging for crop hail damage assessment in potato. *Computers and Electronics in Agriculture, 127*, 406–412. https://doi.org/10.1016/j.compag.2016.06.019